

Free-electron maser operation at the 1 GHz/1 keV regime

R. Drori, E. Jerby*, A. Shahadi, M. Einat, M. Sheinin

High-Power Microwave Laboratory, Faculty of Engineering, Tel Aviv University, Ramat Aviv 69978, Israel

Abstract

The paper describes a free-electron maser (FEM) experiment operating in the low-frequency (~ 1 GHz) low-energy (~ 1 keV) regime. The table-top FEM device consists of a non-dispersive parallel-stripline waveguide and a planar folded-foil wiggler. The experimental results show a super-regenerative amplification. Oscillations are observed above a threshold of the wiggler field.

1. Introduction

A typical FEL employs a high-energy electron beam which undulates in a periodic static magnetic field (wiggler) and interacts with a short-wavelength em radiation [1]. The tuning condition of the FEL interaction is

$$\omega \sim \frac{V_z k_w}{1 - V_z/V_{ph}}, \quad (1)$$

where V_z is the average axial electron velocity, ω and V_{ph} are the em wave angular frequency and phase velocity, respectively, and k_w is the wiggler periodicity.

In the relativistic limit ($V_z \rightarrow c$, $V_{ph} = c$), the Doppler up-shift is large and Eq. (1) shows that $\omega \gg V_z k_w$. Hence, the em wave frequency might be much higher than the electron wiggling frequency, and it may reach the visible and the UV regimes. FEL-type devices have also been operated in the mildly relativistic regime, typically in the microwave and the millimeter wave regimes. These devices are known as ubitrons [2] or free-electron masers (FEMs). Unlike short-wavelength FELs which operate in free-space modes, the ubitron-FEMs employ hollow metallic waveguides to guide the long-wavelength radiation in TE or TM modes. Consequently, $V_{ph} > c$, and the Doppler up-shift in Eq. (1) is reduced due to the waveguide effect. In many cases, FEMs employ axial magnetic fields to guide the electron beam.

The experiment described in this paper is conducted with an extremely low electron beam energy, in the order of only 1 keV. This energy is much lower than any other known ubitron-FEM [3]. The device employs a non-dispersive waveguide which supports a TEM-mode propagating at the speed of light, i.e. $V_{ph} = c$, as in the relativistic FELs.

Since the electron beam is extremely slow ($V_z \ll c$), the FEL tuning condition (1) is reduced to

$$\omega \sim V_z k_w. \quad (2)$$

Hence, the Doppler shift is negligible and the radiation frequency is close to the electron wiggling frequency.

2. Experimental setup

A general schematic of the FEM experimental device with the non-dispersive waveguide is shown in Fig. 1. The experimental setup is based on the FEM oscillator experiment [4] conducted at Tel Aviv University. The tube consists of a planar-diode electron gun, a parallel strip-line non-dispersive waveguide, a solenoid, and a planar folded-foil undulator. A low-energy electron beam is injected into the waveguide and interacts with the TEM wave. The electron beam is dumped at the exit of the interaction region onto a collector, which is also used to measure the

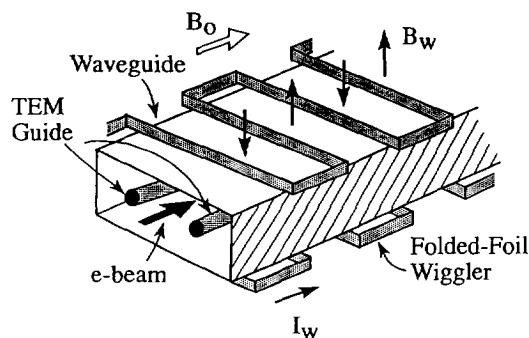


Fig. 1. A scheme of the FEM device in a non-dispersive waveguide.

* Corresponding author. Fax +972 3 6423508, e-mail jerby@tau.nv.tau.ac.il.

Table 1
Experimental parameters

Electron beam	
Energy	~1 keV
Current	<0.5 A
Pulse width	~50 μ s
Magnetic field	
Uniform solenoid	~2 kG
Folded-foil undulator	
Strength	~0.5 kG
Period	2.0 cm
Waveguide	
Rectangular tube	0.9×0.4 in. ²
Parallel wires	
Wire diameter	1.9 mm
Distance between centers	11 mm
Length	48 cm

electron current. The experimental parameters are listed in Table 1.

The static magnetic field is produced in this experiment by a combination of a solenoid and a planar undulator as shown in Fig. 1. The total magnetic field on-axis is given by $B_0 \approx \hat{x}B_w \cos k_w z + \hat{z}B_0$. The electron trajectory is, consequently, a superposition of a wiggling motion and a cyclotron motion. The undulator used in this experiment is a coaxially-fed *folded-foil* wiggler as described in Ref. [5]. The wiggler strength B_w is determined by the current I_w in its windings, according to $B_w = (2\mu_0 I_w N / \lambda_w) \text{sech}(k_w h / 2)$, where N is the number of winding layers, and h is the wiggler gap. In this experiment, $\lambda_w = 2$ cm, $h = 2$ cm, $I_w \leq 550$ A, and $N = 7$. (The first three periods at the ends of the wiggler are tapered.) The maximum wiggler magnetic field on-axis is ~0.5 kG. Three synchronized pulsers generate the solenoid, the e-gun, and the wiggler pulses, as described in Ref. [6]. The e-gun pulser [7] and the high-current wiggler pulser are triggered at the peak of the 20 ms solenoid pulse.

The non-dispersive Lecher-type parallel stripline waveguide shown in Fig. 1 consists of two metal wires along a standard WR90 rectangular tube. The wires are supported by two small ceramic (Macor) holders at the center of the waveguide. The impedance of the coplanar waveguide is ~200 Ω . The waveguide is terminated at the input and the output ports by two tapered adaptors connecting the two-wire Lecher type waveguide to 50 Ω coaxial lines. Cold measurements using a scalar network analyser (HP8757) show that at 1 GHz frequency, the transmission loss is 1.5 dB and the return loss is 10 dB. Thus, the condition for an oscillation build-up in this case is an FEM amplification of more than 20 dB.

Fig. 2 shows the RF diagnostic setup. An RF signal generated by a synthesizer (HP83752A) is split into two arms in an interferometer form. In one arm the signal is amplified by the FEM device. The output signal is attenuated and split into a power detector and a mixer. The

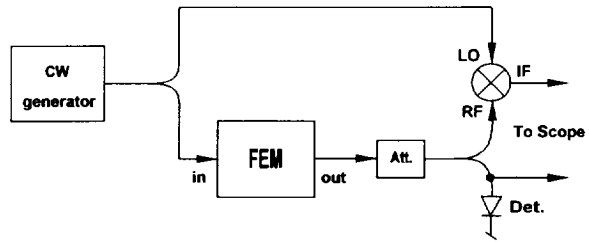


Fig. 2. The microwave diagnostic setup.

local oscillator (LO) is provided by the synthesizer. The detector and the mixer outputs are shown by a Tektronix TDS 540 oscilloscope with the electron beam voltage and current. This setup enables measurements of amplification, super-regenerative amplification, and oscillation build-up, as presented in the next section.

3. Experimental results

Various responses are observed in the FEM experiment in low and high wiggler field strengths. Below a threshold in the wiggler current ($I_w \sim 0.2$ kA), no interaction is observed in this experimental setup. Slightly above this threshold, amplitude and phase variations are measured in the power detector and in the heterodyne mixer, respectively. In higher wiggler currents ($I_w \sim 0.4$ kA), oscillations are built up. Free oscillations are also observed without an external RF injection, though their power levels are typically smaller.

Figs. 3 to 6 show typical measurements of the FEM performance. The electron gun voltage is shown in Fig. 3. During the voltage sweep, variations in the power detector

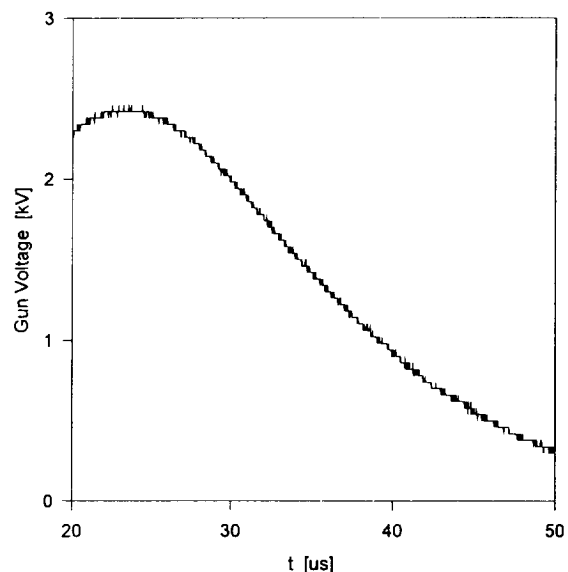


Fig. 3. A typical trace of the electron gun voltage.

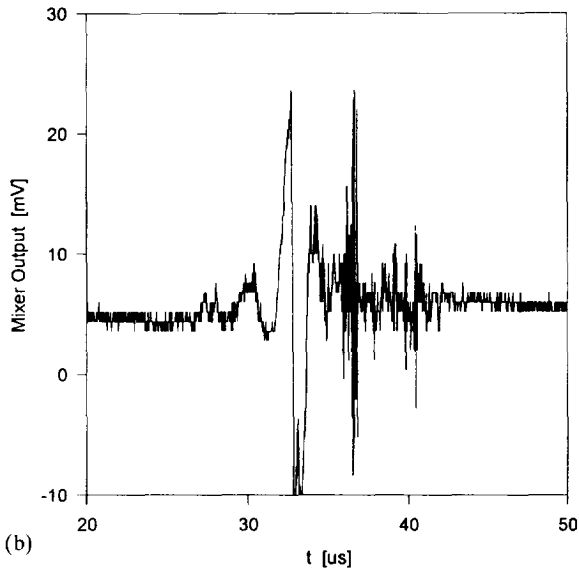
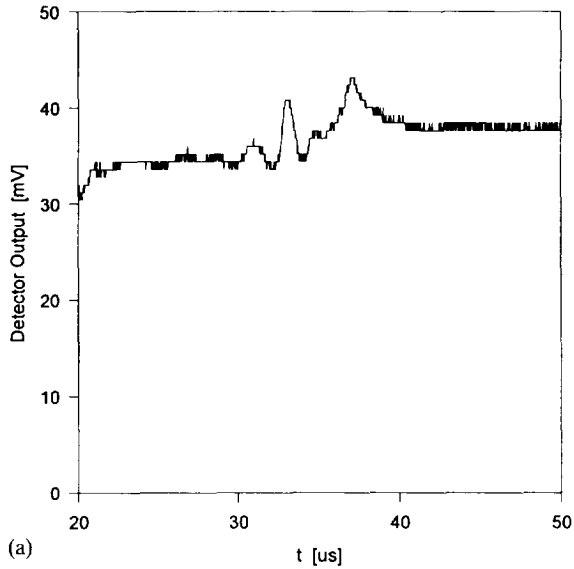


Fig. 4. Measurements with a low wiggler current ($I_w = 0.37$ kA) and a 0.9 GHz input signal. (a) RF-power detector output. (b) Heterodyne mixer output.

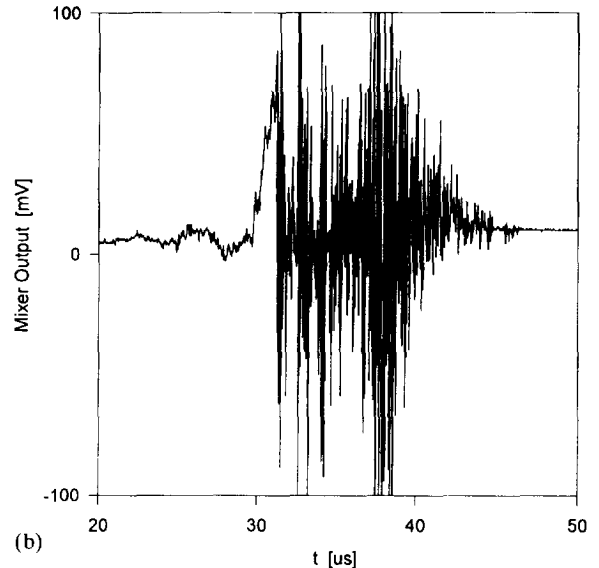
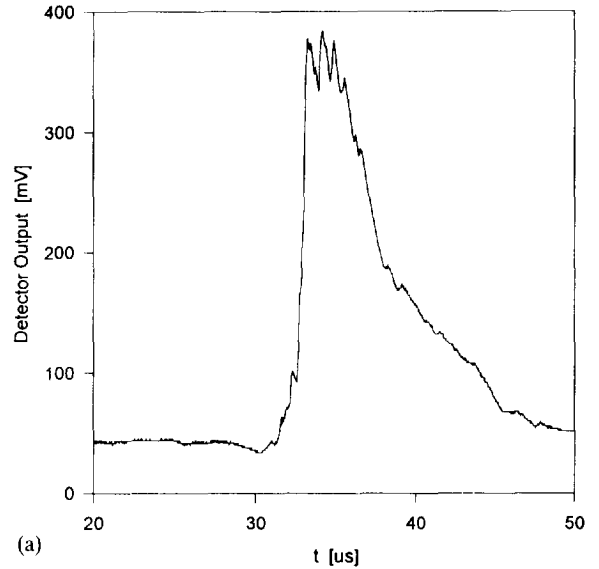


Fig. 5. Measurements with a high wiggler current ($I_w = 0.52$ kA) and a 1.0 GHz input signal. (a) RF-power detector output. (b) Heterodyne mixer output.

level and the heterodyne mixer output are observed in various wiggler levels. Figs. 4a and 4b show the detector and the mixer output signals, respectively, for $I_w = 0.37$ kA and 0.9 GHz input signal. Amplitude and phase variations are clearly observed. A larger wiggler field ($I_w = 0.52$ kA) yields a much stronger response as shown in Figs. 5a and 5b. Oscillations are built up in a mechanism of a super-regenerative amplification near the injected signal frequency (1 GHz) as shown in the heterodyne measurement (Fig. 5b). Under the same conditions, but without an external RF injection, free oscillations are built up to a lower power level as shown in Figs. 6a and 6b. The

experimental results in over 50 runs conducted recently agree with the FEL tuning relation (1) within a $\pm 10\%$ variation range.

4. Conclusions

This experiment demonstrates an FEL type interaction in the frequency-energy range of ~ 1 GHz/ ~ 1 keV. These operating parameters are the lowest known to us in the FEL literature [3].

Our experiment extends the lower limit of the FEL

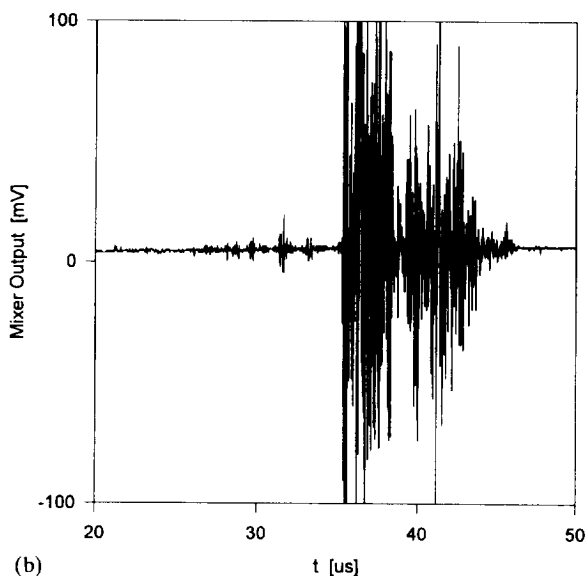
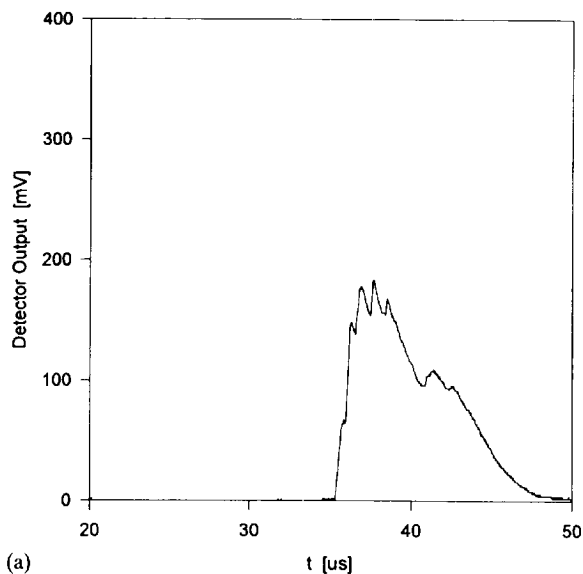


Fig. 6. Measurements of free oscillations with a high wiggler current ($I_w = 0.52$ kA). (a) RF-power detector output. (b) Heterodyne mixer output.

operating frequency toward radio and cellular communication frequencies. Low-voltage FEL-type devices might be useful in these applications as compact high-power amplifiers and oscillators.

Considering the experimental results presented in this paper, and in light of the possible applications of this new FEL concept, our plans for future studies include (a) an improvement of the impedance matching of the coplanar waveguide, (b) theoretical and experimental studies of the amplification mechanism and possible absolute instabilities in this scheme, and (c) a design of a miniature version of this experimental device.

Acknowledgements

This work is supported in part by the Israeli Ministries of Energy and Science, the Belfer Center of Energy Research, the Israeli Academy of Science, and the Shechterman Foundation.

References

- [1] H.P. Freund and T.M. Antonsen, *Principles of Free-Electron Lasers* (Chapman and Hall, London, 1992) and references therein.
- [2] R.M. Phillips, *IRE Trans. Electron Devices* ED-7 (1960) 231.
- [3] H.P. Freund and V.L. Granatstein, *Nucl. Instr. and Meth. A* 358 (1995) 551.
- [4] R. Drori, E. Jerby and A. Shahadi, *Nucl. Instr. and Meth. A* 358 (1995) 151.
- [5] A. Sneh and E. Jerby, *Nucl. Instr. and Meth. A* 285 (1989) 294.
- [6] E. Jerby, A. Shahadi, V. Grinberg, V. Dikhtiar, M. Sheinin, E. Agmon, H. Golombek, V. Trebich, M. Bensal and G. Bekefi, *IEEE J. Quantum Electron.* QE-31 (1995) 970.
- [7] V. Grinberg, E. Jerby and A. Shahadi, *Nucl. Instr. and Meth. A* 358 (1995) 327.